

Multiplicity distribution and mechanisms of the high-energy hadron collisions

S. G. Matinyan* and W. D. Walker

Department of Physics, Duke University, Durham, North Carolina 27708-0305

(Received 5 January 1998; published 11 January 1999)

We discuss the multiplicity distribution for the highest accessible energies of pp and $\bar{p}p$ interactions from the point of view of multiparton collisions. The inelastic cross sections for single σ_1 and multiple (double and, presumably, triple) σ_2 parton collisions are calculated from the analysis of experimental data on the multiplicity distribution up to Fermilab Tevatron energies. It is found that σ_1 becomes energy independent while σ_2 increases with \sqrt{s} for $\sqrt{s} \geq 200$ GeV. The observed growth of $\langle p_\perp \rangle$ with multiplicity is attributed to the increasing role of multiparton collisions for the high-energy $\bar{p}p(pp)$ -inelastic interactions. σ_{2+3} reproduces quite well the cross section for minijet production. [S0556-2821(99)02403-0]

PACS number(s): 13.85.Hd

I. INTRODUCTION: Koba-NIELSEN-OLESEN SCALING AND ITS VIOLATION

The experimental observations of the violation of Koba-Nielsen-Olesen (KNO) scaling [1] at high-energy (pp) and ($\bar{p}p$) collisions [2] and of the correlations between the average transverse momentum $\langle p_\perp \rangle$ and the multiplicity N of the secondaries (a higher $\langle p_\perp \rangle$ for high multiplicity events) [3] indicate that there are at least two mechanisms of high-energy multiparticle production which exhibit the quark-gluon structure of hadrons and their interactions.

That KNO scaling should be violated at very high energies was realized long ago [4], in the same year when KNO scaling was introduced. This deviation from a KNO type distribution of secondaries was attributed to the possibility of splitting each of the colliding hadrons into several constituents (valence quarks, gluons) pairwise interacting with their counterparts from oppositely moving hadrons. The above picture results in the production of several showers and, in the Regge picture, each shower corresponds to the cut Regge poles in the elastic amplitude.

Inclusion of such contributions changes the structure of the distribution $\sigma_N/\sigma_{\text{tot}}$ (σ_N is the cross section of the production of N secondary hadrons) at large $\xi = \ln s/s_0$ ($s_0 = 1 \text{ GeV}^2$) leading to the appearance of the additional peaks in the distribution with larger $\langle N_n \rangle$ (here n denotes the number of pairs of the inelastically colliding partons involved in the interaction from the different hadrons). At a given number of cut Pomerons, the scheme takes into account the arbitrary number of elastic rescatterings corresponding to the exchanges of uncut Pomerons.

In the present paper we will use the multiplicity distribution data obtained from $p\bar{p}$ colliders for $\sqrt{s} \geq 200$ GeV, including new data from experiment E735 at $\sqrt{s} = 1.8$ TeV, for an estimation of the inelastic cross sections of the soft single (σ_1) and double (σ_2) parton collisions. We describe this analysis in Sec. III. Since our analysis confirms several salient features of the common theoretical picture, we first describe in short the consequences of the dual parton model

(DPM) [5] which provides a comprehensive phenomenological framework for a quantitative description of the numerous properties of the soft processes at high energies and serves as a link between QCD and soft hadron physics. DPM includes as an important component the Regge picture which we used above.

In Sec. II we give a short survey of the treatment of the multiparton inelastic collisions and their cross sections. We give the topological cross sections $\sigma(N, s)$, inelastic parton collision cross section σ_n , where n denotes the number of parton collisions, and describe the characteristic features of the multiplicity distribution and the correlation between $\langle p_\perp \rangle$ and multiplicity. Section III is devoted to the analysis of the data on multiplicity distribution aimed at the estimation of σ_1 and σ_2 . Section IV concludes our analysis and contains some speculations on the high-energy behavior of the soft single and multiple parton inelastic collisions.

II. MULTIPLE COLLISIONS OF PARTONS IN THE DUAL PARTON MODEL (DPM)

Before we describe our analysis (Sec. III) of the data on the multiplicity distribution for $\sqrt{s} \geq 200$ GeV, we briefly discuss here the treatment of the soft processes based on DPM [5] which incorporates the large $N_c(N_f)$ which is the number of the colors (flavors) in a unitarized topological expansion, the concept of the duality, unitarity, parton structure of hadrons, and Regge scheme. To our knowledge, DPM is the only known reliable model which links QCD with the physics of the soft processes and provides a complete phenomenological framework for a quantitative description of the numerous characteristics of the soft processes (for hadron-hadron, photon-hadron, photon-photon, hadron-nucleus, and nucleus-nucleus collisions). As we remarked, the DPM includes the parton structure of hadrons, i.e., the necessary knowledge of the x and p_\perp distribution of the partons inside a hadron. As this information was implemented many times in the older and more recent literature [5], we confine ourselves here to the final expressions for σ_n and related quantities. We use the version of the DPM proposed and developed by the ITEP group [6–8], the so-called quark gluon string model.

In this version of the DPM the ultra-high-energy interac-

*Also at Yerevan Physics Institute, Yerevan, 375036 Armenia.

tion between hadrons, phenomenologically described by Pomeron exchange, is treated as a result of a gluon pair exchange between the constituents of hadrons as they pass close to one another [9]. After a color exchange between constituents (valence quarks, gluons, sea $q\bar{q}$) carried by the colliding hadrons, partons from one hadron are joined by pairs of the gluon strings with partons of the other hadron. When hadrons separate after the collision, a pair of strings is stretched and breaks into the two chains of hadrons. Graphically, this corresponds to the unitary cut of the single dual Pomeron having in DPM the topology of a cylinder [5]. Similarly, a cut in the multi-Pomeron exchange diagram through n Pomerons gives $2n$ chains which attach to the components of the initial hadrons. There exists a one-to-one correspondence between the picture of the gluon strings of the DPM and the soft Pomeron phenomenology, at least in the quasieikonal approximation. As shown in Ref. [8], the gluon string model (or DPM) leads to the same expression for a variety of the quantities characterizing the high-energy soft collision as does the Regge diagram technique, giving also the possibility to determine some of the free parameters of the last one.

In the present paper we describe the “soft” $p\bar{p}$ collisions which constitute the bulk of the events in the final state, using the DPM which effectively comes to the soft Pomeron picture. In this picture a single cut Pomeron gives the dominant contribution to the inelastic cross section and this corresponds to the single parton-parton collision resulting in the mean hadron multiplicity $\langle N_1 \rangle$. We assume, in accordance with the Introduction [4], that single $pp(\bar{p}p)$ inelastic collisions obey KNO scaling.

Double (and multiple) collisions lead to the violation of KNO scaling and to the double (multiple) mean multiplicity $\langle N_n \rangle = n \langle N_1 \rangle$ where n is the number of soft inelastic parton-parton collisions. Since KNO scaling is well satisfied for the CERN Intersecting Storage Rings (ISR) energy domain and, according to our assumption, to obtain $\langle N_1 \rangle$ we will use mainly the corresponding multiplicity data in the range \sqrt{s} from 11.5 to 62.6 GeV which are well described by the effective single Pomeron exchange. The data at $\sqrt{s} = 200$ GeV which are dominated by single collisions were added to fit to remove the effect of double collisions.

We describe $\langle N_1 \rangle$ for the single inelastic soft collision as $a + b \ln(s/s_0)$ ($s_0 = 1 \text{ GeV}^2$) and find the coefficient a and b from these data [10].¹ As a result of the fit, we have for the coefficients a and b : $a = -7.3$, $b = 2.56$ with $\chi^2 = 7.085/7$. We have also determined $\langle N_1 \rangle$ from the position of the peak in $d\sigma/dN$. This gives slightly different coefficients.

It is important to remark that the picture we are describing corresponds to the scenario where only “nonenhanced” Regge diagrams are included in the scattering amplitude (“quasieikonal” approximation). “Enhanced” diagrams where the branching of chains ladders is possible, lead to the

smearing out of the distribution between the peaks of the multiplicity distribution thereby reducing the effects of KNO violation. There are arguments that the “enhanced” diagrams have a small effect. The strong violation of KNO scaling (in the whole rapidity interval) at highest achievable energies ($\sqrt{s} \geq 500 \text{ GeV}$) is one more argument supporting the smallness of the “enhanced” graphs.

Since the distributions of particles from different chains are independent in first approximation, one can expect that the width of the multiplicity distribution for multiple collisions obey the rule $\Delta N_n \sim \sqrt{n \langle N_1 \rangle} = \sqrt{n} \Delta N_1$ leading to the broadening of the distribution $\sigma_N / \sigma_{\text{inel}}$. If there are no long-range correlations among the particles belonging to one chain ladder, their distribution can be described as Poissonian.

It is important to stress that the multi-Pomeron diagrams are especially important in the treatment of the Pomeron as a pole with intercept $\alpha(0)$ higher than unity [$\alpha(0) = 1 + \Delta$; for “soft” interaction $\Delta \approx 0.08$ as experimental data show]. The role of the multi-Pomeron contribution to the σ_{tot} and σ_{inel} is increased with energy [7]. The contribution of Pomerons to σ_{tot} is $\sim e^{n\Delta\xi}$, the effective number of cut Pomerons (in the “quasieikonal” treatment) $n_{\text{eff}} \sim e^{\xi_n \Delta}$ ($\xi_n = \ln s/s_0 n^2$) [7] which is ~ 2.5 for $\sqrt{s} \leq 2 \text{ TeV}$ ($n=2$). Thus from our point of view, only double “soft” inelastic parton collisions, in addition to the single ones, are expected up to Tevatron energy. In the LHC domain ($\sqrt{s} = 14 \text{ TeV}$) this parameter $n_{\text{eff}} \approx 3.3$ ($n=3$), indicating the possibility of the appearance of the third maximum in $\sigma_N / \sigma_{\text{inel}}$ distribution at $\langle N_3 \rangle \approx 3 \langle N_1 \rangle$. This pattern is presented below (see Figs. 1 and 2) where we calculated σ_n , the inelastic cross sections corresponding to the n -fold parton collisions which here, according to the ideas of DPM, correspond to the contribution of n cut Pomerons, accompanied by the exchange of the arbitrary number of uncut Pomerons (quasielastic rescatterings), to the scattering amplitude.

We briefly outline the main steps leading us to Figs. 1 and 2 which are discussed in the literature [6–8]. We are interested in the inelastic topological cross sections $\sigma_{\text{inel}}(N, S)$ not including the single diffraction dissociation (NSD).

We can write, for $\sigma_{\text{inel}}(N, s)$,

$$\sigma_{\text{inel}}(N, s) = \sum_{n=1}^{\infty} \sigma_n P(N, \langle N_n \rangle), \quad (1)$$

where $P(N, \langle N_n \rangle)$ is the distribution of the N produced particles (in full phase space) in the $2n$ shower events (corresponding to n -fold parton collision). Here, according to our picture, $\langle N_n \rangle = n[a + b \ln(s/s_0 n^2)]$. $\sigma_n(\xi_n)$ is the cross section for the simultaneous production of $2n$ chains which were created in n -fold parton collisions [$\xi_n = \ln(s/s_0 n^2)$]. $\sigma_n(\xi_n)$ is obtained by the unitary cuts of n Pomerons accompanied by an arbitrary number of elastic rescattering (no cut Pomerons) [6,8].

To trace the trends of the multiplicity distribution and reveal the role of multiparton collisions, we take for $P(N, \langle N_n \rangle)$ the Poisson distributions for the number of pairs

¹When the present paper was written we became aware of the recent similar treatment of the average multiplicity $\langle N_1 \rangle$ as a linear logarithmic function for the soft component [11].

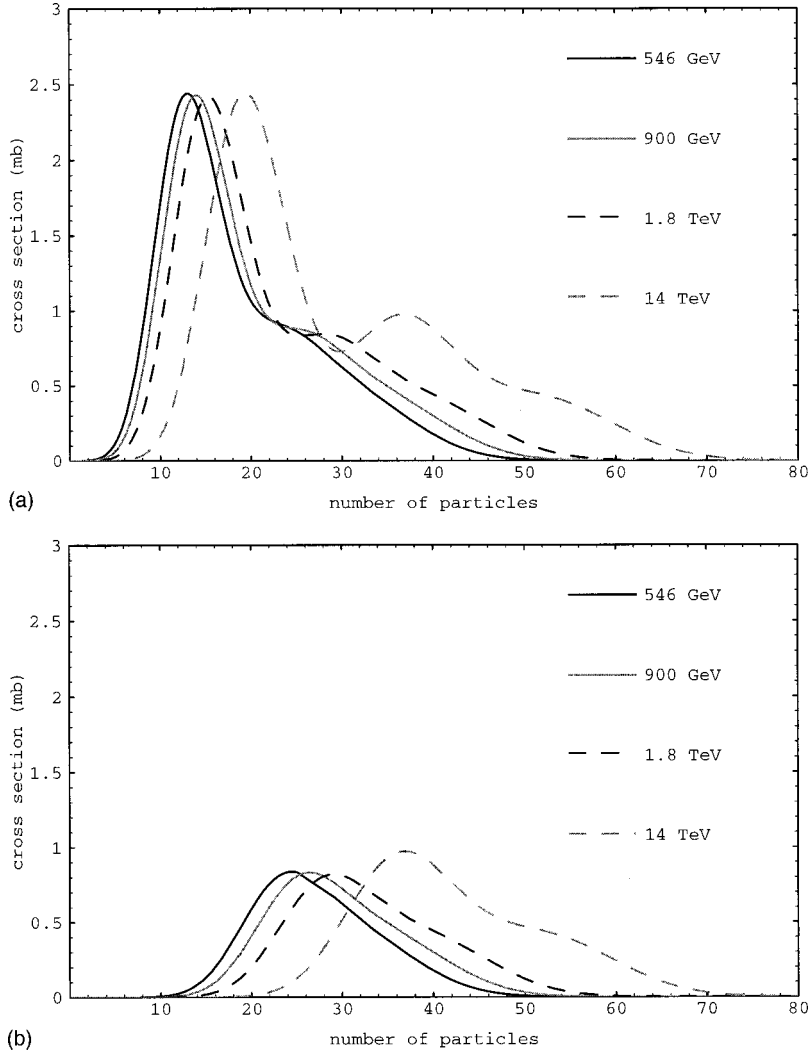


FIG. 1. (a) Topological cross sections σ_N in the quasiclinal approximation with exchanges of three effective “soft” Pomerons for $\sqrt{s} = 546, 900, 1800,$ and 14×10^3 GeV. (b) Topological cross sections resulting from double and triple parton collisions for $\sqrt{s} = 546, 900, 1800,$ and 14×10^3 GeV.

of charged particles. Then, summing over N in Eq. (1) and taking into account that $\langle N_1 \rangle$ is always large, we can write

$$\sigma_{in}^{NSD}(s) = \sigma_1 + \sigma_2 + \sigma_3 + \dots \quad (2)$$

This relation, of course, does not depend on the concrete form of $P(N, \langle N_n \rangle)$.

For $\sigma_n(\xi_n)$ we have [6,8]

$$\sigma_n(\xi_n) = \frac{\sigma_P}{n Z_n} \left(1 - e^{-Z_n} \sum_{k=0}^{n-1} \frac{Z_n^k}{k!} \right), \quad (3)$$

with

$$\sigma_P = 8\pi\gamma_P \left(\frac{s}{s_0} \right)^\Delta, \quad Z_n = \frac{2C\gamma_P}{R^2 + \alpha'_p \xi_n} \left(\frac{s}{s_0 n^2} \right)^\Delta. \quad (4)$$

The parameters in these expressions are fixed by the fits of the experimental data on σ_{tot} and $d\sigma_{el}/dt$ for pp and $\bar{p}p$ collisions [7,8]:

$$\gamma_P = 3.64 \text{ (GeV)}^{-2}, \quad R^2 = 3.56 \text{ (GeV)}^{-2}, \quad C = 1.5,$$

$$\Delta = \alpha_p(0) - 1 = 0.08,$$

$$\alpha'_p = 0.25 \text{ (GeV)}^{-2}, \quad s_0 = 1 \text{ (GeV)}^2. \quad (5)$$

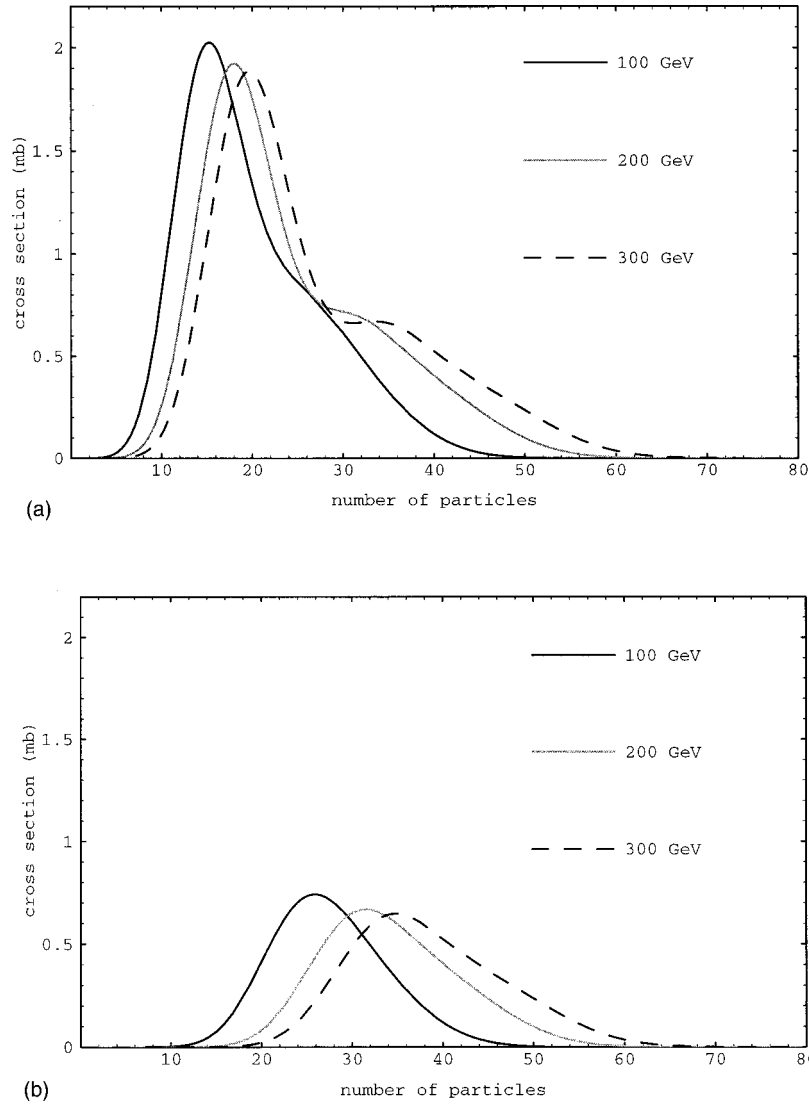
We would like to mention that that scheme, due to the multi-Pomeron exchanges, is unitary and asymptotically satisfies the Froisart bound [7,8]

$$\sigma_n(\xi_n) \approx \xi_n \text{ at } \xi_n \gg 1, \quad n \text{ not large,}$$

$$\sigma_{tot} \sim s^{0.08} (\xi \Delta \leq 1),$$

$$\sigma_{tot} = 2\sigma_{in} = \sum_{n=0}^{\infty} \sigma_n(\xi) = \sigma_P f(Z/2)$$

$$\approx \frac{8\pi\alpha'_p\Delta}{C} \xi^2 \text{ for } \xi \Delta \gg 1. \quad (6)$$

FIG. 2. Same in Fig. 1 for $\sqrt{s}=100, 200,$ and 300 GeV.

Here

$$f(Z) = \sum_{\nu=1}^{\infty} \frac{(-Z)^{\nu-1}}{\nu \nu!} = \frac{1}{Z} \int_0^Z (1 - e^{-x}) \frac{dx}{x} = \frac{1}{Z} [\Gamma(0, Z) + \ln(\gamma_E Z)] \quad (7)$$

with $\gamma_E = 1.78 \dots$ the Euler constant and $\Gamma(\alpha, Z)$ -incomplete gamma function, $Z = Z_1$.

As concerns the multiplicity, for the single collisions, only $\langle N_1 \rangle$ has a simple logarithmic dependence $\langle N_1 \rangle \approx 2\xi$ at high energies ($\xi \Delta \gg 1$). This fact justifies our choice to define $\langle N_n \rangle$ as $n \langle N_1 \rangle$ for small n .

These formulas (2)–(5) give reasonable estimates of the size of the cross sections for double and, possible, triple collisions. As we will see below, they fail to give a good description of the energy dependence of the double collision cross section σ_2 . There must be a correlation function $F(x_1, x_2)$ which gives the probability of finding partons with

momentum fraction x_1, x_2 essentially simultaneously in the nucleon. This is not included in the scheme.

In Fig. 1(a) we show the N distributions of $\sigma_{in}(N, s)$ at $\sqrt{s} = 0.55, 0.9, 1.8,$ and 14 TeV. At lower energies the second peak of $\sigma_{in}(N, s)$ is not resolved. Figure 1(b) shows the behavior of the parts of $\sigma_{in}(N, s)$ which corresponds to the double and triple collisions.

In Table I we present values of the inelastic ‘‘partial’’ cross sections $\sigma_1, \sigma_2,$ and σ_3 corresponding to the single,

TABLE I. Values of the inelastic cross sections for the single (σ_1), double (σ_2), and triple (σ_3) parton collisions in the Regge quasieikonal model.

\sqrt{s} , TeV	σ_1 , mb	σ_2 , mb	σ_3 , mb	$\sigma_1 + \sigma_2 + \sigma_3$, mb
0.55	21.94	9.57	5.25	36.76
0.9	22.72	10.16	5.71	38.59
1.8	23.84	10.72	6.34	40.90
14	27.19	14.70	8.43	50.32

double, and triple parton collisions in the Regge quasieikonal approximation. We see that in this approach all σ_i ($i = 1, 2, 3$) increase with \sqrt{s} whereas our analysis in Sec. III indicates that the “single” collision contribution σ_1 extracted from the experimental data on the multiplicity distribution practically is independent of \sqrt{s} for $\sqrt{s} \geq 200$ GeV. Furthermore, $\sigma_1 + \sigma_2 + \sigma_3$ are systematically lower than the experimental cross section $\sigma_{in}(s)$ for the nonsingle diffraction events, while the corresponding theoretical values of this cross section resulting from the summation of all quasieikonal Pomeron graphs [7,8]

$$\sigma_{in}(s) = \sum_{n=1}^{\infty} \sigma_n = \sigma_p f(Z) \quad (8)$$

are in excellent agreement with experimental data for σ_{in} .

Figures 2(a) and 2(b) show for completeness the $\sigma(N, s)$ for lower \sqrt{s} (but higher than 62 GeV) ($\sqrt{s} = 100, 200, 300$ GeV). On these figures at $\sqrt{s} = 200$ GeV the shoulder, corresponding to the double collision, is clearly seen.

The DPM, where the double inelastic parton collisions are described by the contribution of the two cut Pomerons to the scattering amplitude, predicts also the increase of the average transverse momentum $\langle p_{\perp} \rangle$ in the soft processes in the regime $p_{\perp} / \sqrt{s} \ll 1$. Indeed, the p_{\perp} dependence of two Pomeron amplitudes is given by $e^{-\lambda_2 p_{\perp}^2 / 2}$ with $\lambda_2 = R^2 + \alpha'(0) \xi_2$, which leads to the ratio

$$\frac{\langle p_{\perp} \rangle}{\langle p_{\perp} \rangle_1} \approx \sqrt{2}$$

in agreement with data. The further increase of the $\langle p_{\perp} \rangle$ can be expected at the effective opening of the triple parton collision which, as we can see from Fig. 1, should be clearly displayed in the CERN Large Hadron Collider (LHC) energy range.

Thus the inclusion of the “soft” double parton collisions leads not only to the higher ($\langle N_2 \rangle \approx 2 \langle N_1 \rangle$) multiplicity (and to the violation of KNO scaling) but also to the correlation between $\langle p_{\perp} \rangle$ and the multiplicity. These two issues are contributed sometime to the increasing role of the “semihard” collisions at higher energies (“minijets”).

From our point of view, the double collisions are “soft” in essence. Moreover, since they are less probably than single ones, we need to arrange the collision at the smaller impact parameters which, together with the increasing role of the double collisions with energy, leads to the larger $\langle p_{\perp} \rangle$ (≈ 0.6 GeV) at higher N and \sqrt{s} .

Of course, one can include the semihard component into the DPM by hand. However, as stressed by the Orsay group [5], (i) in the wide energy range the minijets, in many respects, behave just like a part of the soft multichains, and therefore, are implicitly included in DPM, (ii) a considerable fraction of the rise of σ_{tot} and σ_{in} is due to the soft component, (iii) introduction of a semihard component to account

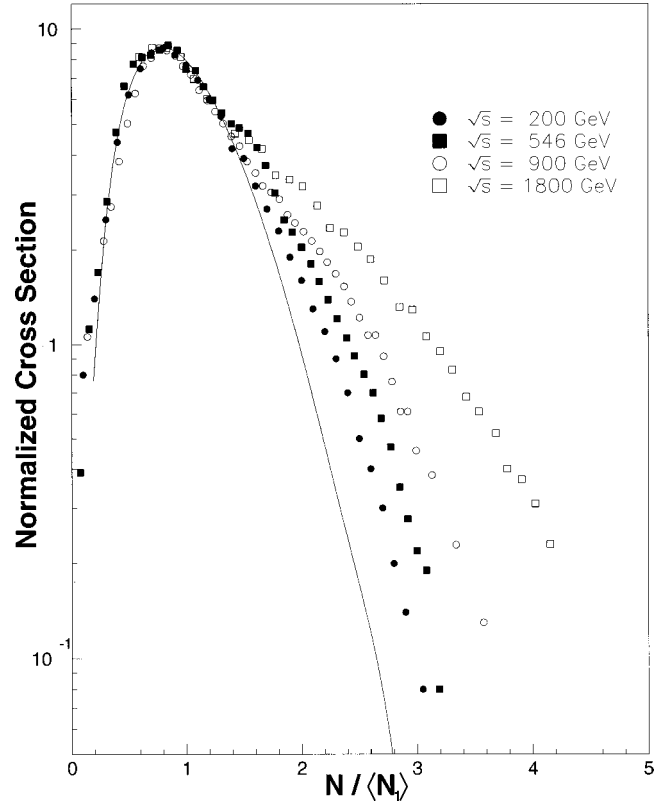


FIG. 3. A comparison of multiplicity distributions at different values \sqrt{s} . The distributions are normalized at the maximum value of $d\sigma/dx$ where $x = N/\langle N_1 \rangle$. The solid curve is the KNO distribution from ISR data.

for the KNO violation shows that they have a small influence, and the DPM mechanism of KNO violation is maintained. The same conclusion holds for the problem of $\langle p_{\perp} \rangle$ correlation with multiplicity. The division of the multiparticle collisions into “soft” and “hard” ones reflects our inability to solve QCD at small p_{\perp} .

III. ANALYSIS OF THE MULTIPLICITY DISTRIBUTION DATA

We now turn to our main goal—to extract σ_1 and σ_2 from the multiplicity distributions. We analyze the data obtained from the energy range \sqrt{s} from 30 to 1800 GeV including ISR, UA5, and Tevatron (E735 experiment) data. As a basis of our analysis, we use the fact that KNO scaling is well satisfied for the experimental data through ISR energies. The deviation from the sample KNO scaling at higher energies is due to another process which is incoherently superimposed on the KNO producing process.

In Fig. 3 the collider data from different energies are superimposed on one plot. The experimental distributions $(1/\sigma_{NSD})(d\sigma/dx)$ have been normalized to the same value of the variable $x = N/\langle N_1 \rangle$ at the x_{max} , at which the corresponding KNO distribution has a maximum. It turns out that this quantity at the maximum and for values of $x \leq 1.3$ is essentially independent of energy.

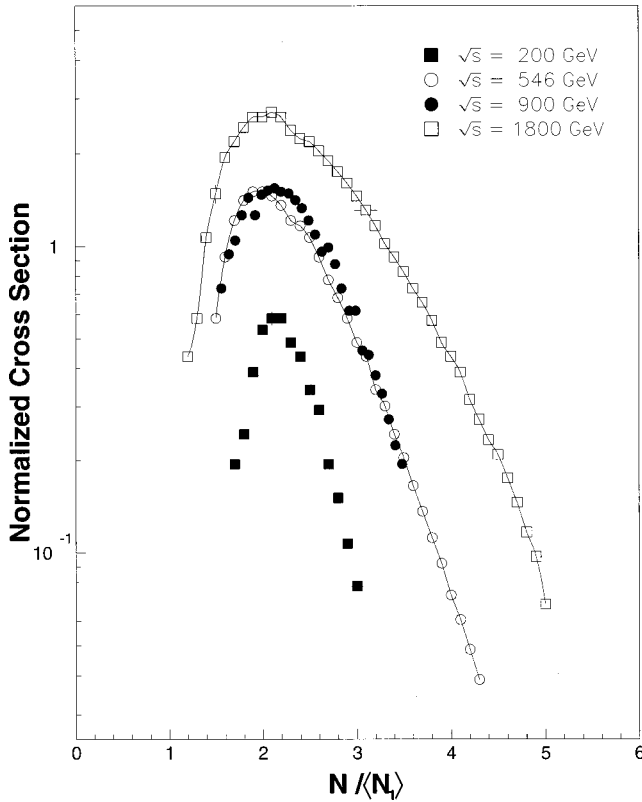


FIG. 4. Multiplicity distributions obtained by taking the difference between the $p\bar{p}$ collider data and the KNO distribution.

From the measurement of the KNO curve at the ISR energies we know that $N_{\max} = 0.8\langle N_1 \rangle$. Thus, we can estimate the value of $\langle N_1 \rangle$, the average multiplicity for the process with pure KNO scaling, at higher energies from the known value of N_{\max} at which the $(1/\sigma_{NSD})(d\sigma/dx)$ is a maximum.

As we remarked above, the deviation from the KNO shape is due to another process which is incoherently superimposed on top of the KNO producing process. By subtracting the KNO distribution from the experimental data we determine the shape of the competing process as shown in Fig. 4. The shapes of the multiplicity distribution thus found are rather different from the KNO shape and is not a simple convolution of the KNO distribution.

The main characteristics of the derived distributions is that the most probable value of the distributions occurs at $x = 2$ [or at twice the multiplicity corresponding to the initial low-energy (single collisions) KNO distribution]. The width of the distribution is close to $\sqrt{2}$ times the width of that KNO shape at $\sqrt{s} = 1800$ GeV. This is in quite good agreement with the picture based on the DPM we presented above, which is based on the adding of the double inelastic collision of partons of the colliding hadrons described by the contribution of two cut Pomerons (or two pairs of gluonic strings) to the single inelastic parton collision described by one cut Pomeron (one pair of gluonic strings).

Independently of the concrete realization of the interaction between ultrarelativistic parton pairs, we interpret the population of the secondaries with a maximum at $2\langle N_1 \rangle$ as a result of two independent (and simultaneous) parton-parton

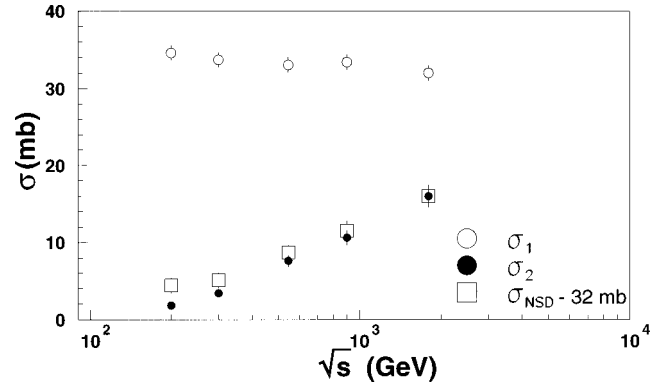


FIG. 5. Cross sections for the single (σ_1) and multiparton (double and triple) (σ_2) parton collisions as a function of \sqrt{s} .

inelastic collisions occurring in the same encounter. Integrating the distributions displayed in Fig. 4 over x we obtain the inelastic cross section σ_2 for the double parton collisions as a function of \sqrt{s} and the inelastic cross section σ_1 for the single parton collision ($\sigma_1 = \sigma_{NSD}^{in} - \sigma_2$) (Fig. 5). The last cross section σ_1 which is characterized by the KNO scaling, as seen from Fig. 5, is nearly independent of \sqrt{s} for $\sqrt{s} \geq 200$ GeV and has a value of (34 ± 2) mb. σ_2 is increased with \sqrt{s} .

The data shown in Fig. 5 seems to reveal an apparent threshold for double collisions \sqrt{s} close to 100 GeV. It may be related to the fact that in these collisions, $\langle N_2 \rangle = 2\langle N_1 \rangle$, $\langle N_1 \rangle \approx 16$ at $\sqrt{s} = 100$ GeV. To produce 32 particles would require essentially all of the center of mass energy.

Before we proceed further, it is worthwhile to spend some time and space to describe the above procedure of estimation of σ_1 and σ_2 in the formal way. We can write for the experimentally observed (normalized to unity) distribution

$$\left(\frac{\langle N \rangle \sigma_N}{\sigma_{NSD}^{in}} \right)_{\text{exp}} = \frac{1}{\sigma_{NSD}^{in}} \left(\frac{d\sigma}{dz} \right)_{\text{exp}} \left(z = \frac{N}{\langle N \rangle} \right). \quad (9)$$

With our assumption of the incoherent sum of the single (KNO scaled) and the double (KNO violating) collision cross sections, we can write

$$\frac{1}{\sigma_{NSD}^{in}} \left(\frac{d\sigma}{dz} \right)_{\text{exp}} = \frac{1}{\sigma_{NSD}^{in}} \left(\frac{d\sigma_1}{dz} + \frac{d\sigma_2}{dz} \right), \quad (10)$$

which leads to

$$\frac{\sigma_2}{\sigma_{NSD}^{in}} = 1 - \frac{\sigma_1}{\sigma_{NSD}^{in}} \equiv a(s). \quad (11)$$

Experimentally, $a(s)$ is increasing with \sqrt{s} (Fig. 3). Therefore,

$$\sigma_1 = \sigma_{NSD}^{in} [1 - a(s)] \quad (12)$$

can be (and it is, as Fig. 5 shows) independent of \sqrt{s} , while

$$\sigma_2 = \sigma_{NSD}^{in} a(s) \quad (13)$$

is definitely increased.

From Fig. 5 we see that σ_2 equals 17 mb at 1.8 TeV, which we can compare with the Collider Detector at Fermilab (CDF) recent value for the effective double-parton collision cross section ($14.5 \pm 1.7 + {}_{-2.3}^{1.7}$) mb [12]. We note that AFS gives for $\sigma_2(\sqrt{s} = 63 \text{ GeV}) \sim 5 \text{ mb}$ [13] while UA2 presents a lower limit 8.3 mb [14]. We remark that in the sample of events the CDF has removed events with possible triple collisions. Our procedure admits the addition to the σ_2 the triple collisions which have small cross sections (see Table I for σ_3) at the Tevatron energy domain.

Some remarks on the experimental data of E735 and UA5 are necessary. In Figs. 3–5 we do not show error bars on all the points in the derived distributions. The statistical errors in E735 are relatively small. However, the systematic error in both experiments might be sizable. In E735 as well as UA5 the multiplicities in a restricted range of rapidity are extended to the full range by computer simulation. There are corrections for secondary interactions in individual events. The derived distributions in Fig. 3 suffer in accuracy from the fact that one subtracts two different distributions which each have uncertainties. When the experimental data and the KNO distribution are close in value then the error is greater. Fortunately, the KNO distribution is only the order of 10–15 % of the experimental data at $N = 2\langle N_1 \rangle$ ($x = 2$) and consequently, the position of the peak in the derived distribution is not strongly affected by errors produced by taking the differences. The whole distribution might move up and down as a result of errors in either of the KNO or experimental distributions. The errors in the value of σ_2 are sensitive to the determination of $\langle N_1 \rangle$ [$\delta\sigma_2/\sigma_2 \approx 3(\delta\langle N_1 \rangle/\langle N_1 \rangle)$]. We can conclude from our analysis that the double (and possibly triple) inelastic parton collisions account for a large fraction of the major part of the total $p\bar{p}$ cross section and, definitely are responsible for the increase of the $p\bar{p}$ inelastic cross section at collider energies ($\sqrt{s} \geq 200 \text{ GeV}$). As the collision energies will increase to LHC values, it seem likely that double and possibly triple collisions will constitute a larger fraction of the inelastic cross section as is seen in our analyses from the previous sections (see Fig. 1).

It is interesting to note that the cross sections of the minijet production extracted from the several experiments [15,16] are very similar, by their \sqrt{s} dependence and by absolute values, to the σ_2 which we obtained; it has a threshold of $\sqrt{s} \approx 200 \text{ GeV}$. Moreover, if we subtract a minijet production cross section from $\frac{2}{3}\sigma_{\text{tot}}$ (which is close to the σ_{NSD}^{in}), one obtains a \sqrt{s} -independent cross section [16] which is equal approximately to our σ_1 and reproduces Fig. 5. One can conclude that the double parton collisions mostly lead to the minijet production.

For us, this coincidence is an additional argument for the Orsay group's claim that the minijets behave in many respects just like a part of the soft component (multichains)

and are implicitly included in DPM (see Sec. II). This similarity also reflects in our opinion, the existence of the smooth transition from hard (jet) to soft physics of the hadron collisions. It is worthwhile, maybe, to remark also that the constancy obtained here of the σ_1 is the basic assumption of the so-called two component model [17] incorporating the soft and semihard collisions.

The last remark is concerned with the size of the proton (nonperturbative in essence) which is introduced in the double parton collisions. If we use the simplifying assumptions about the factorization of the proton's two-body parton distribution of the longitudinal fractional momenta and their relative transverse distance \vec{b} , we can express [18] the double-parton cross section in terms of the single parton collision cross section

$$\sigma_D = \sigma_S^2 \int d^2b F^2(\vec{b}), \quad (14)$$

where $F(\vec{b})$ gives the two parton distribution on their relative transverse distance inside proton and is normalized to unity. Taking for $\sigma_{S,D}$ our $\sigma_{1,2}$ ($\sigma_1 = 32 \text{ mb}$, $\sigma_2 = 17 \text{ mb}$) and for $F(b) = (e^{-b^2/R^2})/\pi R^2$, one obtains for a ‘‘hadronic’’ proton radius, $R = 0.96 \text{ fm}$ which looks as reasonable in the light of the simplifying assumptions.

IV. IN LIEU OF CONCLUSIONS

In this paper we have attempted to isolate and study the inelastic double-parton collision mechanism using the analysis of high-energy multiplicity data. The main result of our analysis of these data is that the nonsingle diffractive inelastic cross section consists of two parts. The first part of the cross section corresponding to the single parton collisions is practically independent of \sqrt{s} for $\sqrt{s} > 200 \text{ GeV}$, whereas the second part of the σ_{NSD}^{in} increases significantly with energy and achieves the value 17 mb at $\sqrt{s} = 1.8 \text{ TeV}$. That part was attributed here to the inclusion in the collision process of the double (and, perhaps some triple) inelastic parton collisions. Thus, the increase of the σ_{NSD}^{in} at high \sqrt{s} is almost entirely due to the multiparton collisions.

On the other hand, we know from experiments at lower energies where the single parton collisions indeed dominate, that σ_{NSD}^{in} is increasing with \sqrt{s} . This indicates that at higher energies $\sqrt{s} > 200 \text{ GeV}$ the inelastic cross section due to the single collision goes to saturation, whereas the double collisions give the increase of σ_{NSD}^{in} . One can go further and conjecture that the same saturation will occur for the part of σ_{in} connected with the double parton collisions at much higher energies whereas the σ_{in} due to the triple collisions will still increase with \sqrt{s} , etc., until asymptotically the total inelastic cross section (without diffractive part) will achieve a constant value $\sigma_{in} = \sigma_1^{(\text{sat})} + \sigma_2^{(\text{sat})} + \dots$. Of course, we cannot say anything about the behavior of σ_{el} and σ_{dif} at this hypothetical limit.

We need to emphasize once more that we effectively used in the present paper the DPM and its main ingredient the “soft” Pomeron as a carrier of the interaction between the partons. For us, the double inelastic parton collisions are resulting also from “soft” interaction. From this point of view, the above similarity in energy dependence of the soft double parton interactions and the minijet production seems interesting and important, shedding light on the problem of transition from the hard to the soft hadron physics.

ACKNOWLEDGMENTS

We are grateful to Berndt Müller for interesting discussions and for reading the manuscript. S.M. acknowledges the useful discussions with Leonid Frankfurt and Eugene Levin. W.W. acknowledges the useful discussion with Francis Halzen. We are pleased to acknowledge the help of Glenn Doki and Dan Cronin-Hennessy in the numerical calculations. This work is supported in part by the U.S. Department of Energy Grant No. DE-FG02-96ER-40945.

-
- [1] Z. Koba, H. B. Nielsen, and P. Olesen, Nucl. Phys. **B40**, 317 (1972).
- [2] UA5 Collaboration, G. J. Alner *et al.*, Phys. Lett. **138B**, 304 (1984).
- [3] UA1 Collaboration, G. Arnison *et al.*, Phys. Lett. **118B**, 167 (1982); **123B**, 115 (1983); E735 Collaboration, T. Alexopoulos *et al.*, Phys. Rev. Lett. **60**, 1622 (1988); Phys. Lett. B **336**, 599 (1994).
- [4] V. A. Abramovskii and O. V. Kancheli, Pisma Zh. Eksp. Teor. Fiz. **15**, 559 (1972) [JETP Lett. **15**, 397 (1972)].
- [5] For the exhaustive review of the intensive development by Orsay group of the DPM beginning from 1979 see the important paper by A. Capella, U. Sukhatme, C.-I. Tan, and J. Tran Thanh Van, Phys. Rep. **236**, 225 (1994); Phys. Rev. D **45**, 92 (1992); A. Capella, J. Tran Thanh Van, and J. Kwiecinski, Phys. Rev. Lett. **58**, 2015 (1987); see also the recent paper, A. Capella, A. Kaidalov, V. Nechitailo, and J. Tran Thanh Van, Phys. Rev. D **58**, 014002 (1998) combining the Orsay and ITEP versions of DMP for the successful description on the hadron multiplicity in deep inelastic scattering (DIS) at the DESY *ep* collider HERA.
- [6] K. A. Ter-Martirosyan, Phys. Lett. **44B**, 377 (1973).
- [7] P. E. Volkovitski, A. M. Lapidus, V. I. Lisin, and K. A. Ter-Martirosyan, Yad. Fiz. **24**, 1237 (1976) [Sov. J. Nucl. Phys. **24**, 648 (1976)].
- [8] A. B. Kaidalov and K. A. Ter-Martirosyan, Yad. Fiz. **39**, 1545 (1983) [Sov. J. Nucl. Phys. **39**, 979 (1984)]; **40**, 211 (1984) [**40**, 135 (1984)].
- [9] F. E. Low, Phys. Rev. D **12**, 163 (1975); S. Nussinov, Phys. Rev. Lett. **34**, 1286 (1975).
- [10] V. V. Ammosov *et al.*, Phys. Lett. **42B**, 519 (1972); M. B. Bialkowska *et al.*, Nucl. Phys. **B110**, 300 (1976); W. M. Morse *et al.*, Phys. Rev. D **15**, 66 (1977); S. Barish *et al.*, *ibid.* **9**, 2689 (1974); A. Firestone *et al.*, *ibid.* **10**, 2080 (1974); J. Whitmore, Phys. Rep., Phys. Lett. **10C**, 273 (1974); C. Bromberg *et al.*, Phys. Rev. Lett. **31**, 1583 (1973).
- [11] A. Giovannini and R. Ugoccioni, in Proceedings of the XXVII International Symposium on Multiparticle Dynamics. Frascati, Italy, 1997, hep-ph/9710361.
- [12] CDF Collaboration, F. Abe *et al.*, Phys. Rev. D **56**, 3811 (1997); Phys. Rev. Lett. **79**, 584 (1997).
- [13] AFS Collaboration, T. Akesson *et al.*, Z. Phys. C **34**, 163 (1987).
- [14] UA2 Collaboration, J. Alitti *et al.*, Phys. Lett. B **268**, 145 (1991).
- [15] W. Scott, in XIII International Conference on High Energy Physics, Berkeley, 1986 (unpublished); See also, M. Jacob and P. V. Landshoff, Mod. Phys. Lett. A **1**, 657 (1986).
- [16] UA1 Collaboration, G. Ciapetti, spokesperson, in *The Quark Structure of Matter*, edited by M. Jacob and K. Winter (World Scientific, Singapore, 1986), p. 455, see Fig. 13.
- [17] T. K. Gaisser and F. Halzen, Phys. Rev. Lett. **54**, 1754 (1985); T. K. Gaisser, F. Halzen, A. D. Martin, and C. J. Maxwell, Phys. Lett. **166B**, 219 (1986); B. Humpert, *ibid.* **131B**, 461 (1983); B. Humpert and R. Odorico, *ibid.* **154B**, 211 (1985); N. Paver and D. Treliani, Nuovo Cimento A **70**, 215 (1982); **73**, 302 (1983); see also, P. V. Landshoff and J. C. Polkinghorne, Phys. Rev. D **18**, 3344 (1978); M. Jacob and P. V. Landshoff, Mod. Phys. Lett. A **1**, 657 (1986).
- [18] See, e.g., G. Callucci and D. Treleani, Nucl. Phys. B (Proc. Suppl.) **71**, 392 (1999).